



## Synthesis of Mesoporous Fe<sub>2</sub>O<sub>3</sub>/SBA-15 and its application for Nickel (II) Ion Adsorption

MARIA ULFA<sup>1</sup> and ARINI MIFTAHUL JANNAH<sup>1</sup>

Chemistry Education Study Program, Faculty of Teacher Training and Education,  
Sebelas Maret University, Jl. Ir. Sutami 36A Surakarta, Central Java-57126, Indonesia.

\*Corresponding author E-mail: ulfa.maria2015@gmail.com

<http://dx.doi.org/10.13005/ojc/340145>

(Received: November 05, 2017; Accepted: December 09, 2017)

### ABSTRACT

The uniform mesoporous Fe<sub>2</sub>O<sub>3</sub>/SBA-15 has been successfully synthesized by classical impregnation of iron nitrate acid in the presence of mesoporous silica SBA-15 followed by ultrasonication, microwave treatment and calcination. The characterization of mesoporous Fe<sub>2</sub>O<sub>3</sub>/SBA-15 material structures using FTIR spectroscopy, powder X-Ray Diffraction, Nitrogen adsorption-desorption, Transmission Electron Microscopy, and Energy Dispersive X-Ray (EDX). The result of FTIR analysis showed that mesoporous Fe<sub>2</sub>O<sub>3</sub>/SBA-15 silica material sieves had silanol (Si-OH), siloxyl (Si-O-Si), and Fe-O, while the XRD analysis showed that iron oxide was completely impregnated on mesoporous silica SBA-15 surface. Nitrogen adsorption-desorption analysis showed that surface area of mesoporous Fe<sub>2</sub>O<sub>3</sub>/SBA-15 material was 479 m<sup>2</sup>/g with volume of 0.87 cm<sup>3</sup>/g, and a pore diameter of 6.50 nm. Adsorption Performance of Fe<sub>2</sub>O<sub>3</sub>/SBA-15 material investigated by using nickel (II) ions as adsorbate model. The optimum contact time result was analyzed with adsorption kinetics model. The optimum contact time of adsorption of Fe<sub>2</sub>O<sub>3</sub>/SBA-15 mesoporous material to Ni (II) ion was 240 min. with optimum adsorption capacity of 352.982 mg/g. The optimum contact time data shows that the Fe<sub>2</sub>O<sub>3</sub>/SBA-15 silica mesoporous material in adsorption of nickel (II) ions follows the Lagergren kinetic model.


**Keywords:** Mesoporous silica SBA-15, Iron oxide, Wet impregnation, Ultrasonic, Microwave, Adsorption, Nickel ions

### INTRODUCTION

Nickel is one of the toxic metals cause water contamination. The source of nickel pollution is industrial processes such as electroplating, galvanization, plastics manufacturing, metal finishing, batteries manufacturing, mining, and

dyeing operations<sup>1,2</sup>. The normal level of nickel concentration that permissible in water environment is at range 0.05-0.12 mg/m<sup>3</sup>. The concentration that higher than normal level causing kidney, headaches, stomachache, hepatitis as several problem of health. Conventional methods for the removal Ni (II) from wastewaters has been widely



This is an  Open Access article licensed under a Creative Commons Attribution-NonCommercial-ShareAlike 4.0 International License (<https://creativecommons.org/licenses/by-nc-sa/4.0/>), which permits unrestricted NonCommercial use, distribution and reproduction in any medium, provided the original work is properly cited.

performed by researchers include ion-exchange<sup>3</sup>, electro dialysis and electrocoagulation<sup>4</sup>, floatation<sup>5</sup>, coagulation and flocculation<sup>6</sup>, membrane technology<sup>7</sup>, biofiltration method<sup>8</sup> and adsorption<sup>9</sup>. In general, the high value of method evaluated by a number of requirement such as remove major and minor wastes, low cost, simple and green for environment. From several method, the favourable method for minimize metal ion in water is adsorption. A lot of previous report using adsorption method succes to remove metal ion of cadmium, mercury, iron, barium and toxic molecules of fenol, tiophene, naphtalene and dibenzotiophene

In special case for removing nickel ion, there are many of adsorbent carbon, silica, agricultural, microbes, and chitin<sup>10-15</sup>. The new economic material with not only high sustainability but also has a high adsorption capacity urgently to develop in this decade as a solution for the environmental problem. Currently, mesoporous silica materials attract attention by researchers because it has many advantages such as a high thermal stability, uniform structure, large diameter, high specific surface area and rich with silanol on the framework<sup>11-17</sup>. The most unique of mesoporous silica is mesoporous silica SBA-15 due to the honeycomb shape structure with diameter size up to 15 nm, pore volume up to 1.5 cm<sup>3</sup>/g and specific surface area up to 2500 m<sup>2</sup>/g<sup>12-19</sup>. The mesoporous SBA-15 material silica sieves can be applied in various fields such as adsorption, separation, and catalysis<sup>14-22</sup>. In the adsorption/desorption process, controlling process of the mesoporous silica SBA-15 material showed good thermal stability, physical stability and structural homogeneity<sup>15-23</sup>. In the other side, the mesoporous silica SBA-15 have problem in separation process. When the mesoporous silica SBA-15 have been adsorbed metal ion, it need special treatment to recover SBA-15 from adsorbate. One of favourable separation method is using magnetic component due to the efficiency, not time consuming and economic reason. In the best of our knowledge, the investigation of SBA-15 material in separation section after adsorption process using magnetic element is rarely done.

In our present work, we try to add magnetic element in the mesoporous silica SBA-15. The modification on mesoporous wall-surface was

carried out by doping the iron with the magnetic characteristic. We choose iron as magnetic element to dispersed into the mesoporous silica SBA-15 due to the available stock reason and high magnetic character on it. The objective of this research was to synthesize of adsorbent mesoporous silica SBA-15 (Fe<sub>2</sub>O<sub>3</sub>/SBA-15) modified with iron as metal doping for Ni (II) adsorption using collaboration methods such as wet impregnation, ultrasonic, and microwave. The characteristic of materials was analyzed using FTIR, XRD, BET, TEM, and EDX. We hope can get some information about character of the mesoporous silica SBA-15 modified by iron metal for future magnetic separation material.

## EXPERIMENTAL

### Materials

SBA-15 (pore diameter 7-9 nm, surface area 560 m<sup>2</sup>/g, pore size 8 nm, pore volume 1.0 cm<sup>3</sup>/g and the pore morphology is hexagonal) merk six c materia (China supplier), Fe(NO<sub>3</sub>)<sub>3</sub>·9H<sub>2</sub>O (Merck, pro, analysis), HNO<sub>3</sub> (Merck, 65%), HCl (Merck, 37%), and standard solution of Ni (II) (Merck, 1000 ppm).

### Preparation of Fe<sub>2</sub>O<sub>3</sub>/SBA-15

The activation process of SBA-15 was performed by adding 1.5 g of SBA-15 into the 1 M HCl solution followed by stirring for 24 h in 100 rpm in room temperature. The white slurry filtering with Whatman paper, washing with deionization water and drying at 100 °C for 24 hours. The wet impregnation process was preformed by mixing a fix amount of Fe(NO<sub>3</sub>)<sub>3</sub>·9H<sub>2</sub>O solution as the precursor of the iron ion and 1 g of the activated SBA-15 to obtain 2 wt % Fe on the prepared SBA-15. The material was dispersed by ultrasonication for 1 h and microwave for 30 min. with high temperature labeled Fe<sub>2</sub>O<sub>3</sub>/SBA-15.

### Characterization of Fe<sub>2</sub>O<sub>3</sub>/SBA-15

FTIR spectra of Fe(NO<sub>3</sub>)<sub>3</sub>, SBA-15, and Fe<sub>2</sub>O<sub>3</sub>/SBA-15 were recorded on Shimadzu Shimadzu Corp. Prestige-21. XRD analysis of SBA-15 and Fe<sub>2</sub>O<sub>3</sub>/SBA-15 was performed using Rigaku Multiflex 0.64 kW. The samples were scanned at a 2θ diffraction angle which small angle starts from 2-5 ° and a wide angle starts from 10-80°. The BET SBA-15 and Fe<sub>2</sub>O<sub>3</sub>/SBA-15 such as surface area, volume, and pore diameter were

analyzed using Quantacrome Nova 1200. For morphology of  $\text{Fe}_2\text{O}_3/\text{SBA-15}$  was observed under transmission electron microscope. For the elements contained in the samples were calculated using EDX TSL Ametek with detector type: Sdd Apollo X dan resolution:127.89.

### Adsorption of Ni (II) ions on $\text{Fe}_2\text{O}_3/\text{SBA-15}$

Adsorption experiments have been done with the batch mode in the sample bottle. The standard solution prepared with diluted 1000 ppm solution of Ni (II) 0.05 mol  $\text{HNO}_3$  in  $\text{L}^{-1}$ . The 49 ml solution of Ni (II) contacted with 0,02 g adsorbent  $\text{Fe}_2\text{O}_3/\text{SBA-15}$  and subsequently stirred at room temperature. The experiment was conducted on different adsorption times that is 5-840 min. every sample was taken each of 4 ml of 59 ml solution of Ni (II) using a syringe and filtered through Whatman paper. Finally, the obtained filtrate was measured using AAS (Shimadzu AA 6650). The amount of Ni (II) adsorbed at time  $t$  by  $\text{Fe}_2\text{O}_3/\text{SBA-15}$  using to obtain adsorption capacity. Its investigated by balancing mass calculation.

$$q_e = \frac{C_o - C_e}{w} V \quad (1)$$

The initial and final concentration of nickel ion at time represented by  $C_o$  and  $C_e$  ( $\text{mg}\cdot\text{L}^{-1}$ ). The volume of nickel ion at time (ml) represented by  $V$  and the adsorption capacity of nickel ion represented by  $q$

## RESULT AND DISCUSSION

Figure. 1 show the IR spectra of  $\text{Fe}_2\text{O}_3/\text{SBA-15}$  as adsorbent. The adsorption band at  $676.08 \text{ cm}^{-1}$  and  $1384 \text{ cm}^{-1}$  was attributed to the iron oxide and nitrate ion (Fig. 1a). This is means that material in  $\text{Fe}_2\text{O}_3/\text{SBA-15}$  containing some iron oxide as loading effect and the less number of nitrate ion that can not remove during calnsination. The vibration adsorption peak of the silanol Si-OH bond, which was originally located at  $1639, 56 \text{ cm}^{-1}$  and siloxane Si-O-Si bond at  $1085 \text{ cm}^{-1}$  (Fig. 1b). Fig. 1c, shows the absorption peak of the Si-OH band at  $1635.71 \text{ cm}^{-1}$  and Si-O-Si band at  $1084.04 \text{ cm}^{-1}$ . The peak of silanol and siloxane suggested that the framework of mesoporous silica SBA-15 was quite stable after all step preparation process. However, the vibration peak of the Fe-O band at  $600 \text{ cm}^{-1}$  is disappeared which indicated the

iron-doped within SBA-15 in low number. All the FTIR result not different compare with IR spectra of mesoporous silica SBA-15 and iron in previous report<sup>20</sup>. This phenomenon means that iron modified in the surface of mesoporous silica SBA-15 has been succesfull synthesis in this work.

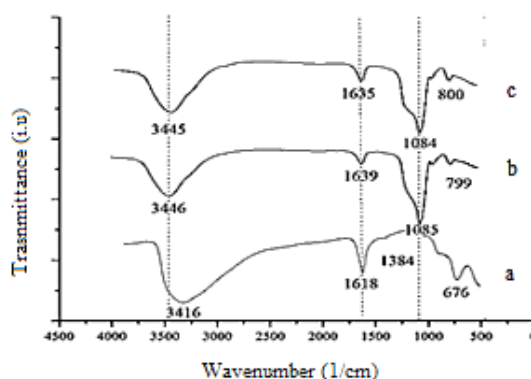


Fig. 1. IR spectra for (a)  $\text{Fe}_2\text{O}_3$ , (b) SBA-15, (c)  $\text{Fe}_2\text{O}_3/\text{SBA-15}$

Diffraction patterns for  $\text{Fe}_2\text{O}_3$ , SBA-15, dan  $\text{Fe}_2\text{O}_3/\text{SBA-15}$  are shown in Fig. 2. that SBA-15 showed two typical diffraction peaks on the reflection (0 1 2) and (1 1 0) at  $2\theta$   $25.5^\circ$  and  $33.5^\circ$ . The small angle diffraction pattern (not shown) describe a typical mesoporous peak by samples at  $2\theta = 1.05^\circ$ . The sample assynthesis  $\text{Fe}_2\text{O}_3/\text{SBA-15}$  shows three reflection peaks (1 0 0), (110) and (2 2 0), this peaks has the similar mesoporous hexagonal structure as SBA-15.  $\text{Fe}_2\text{O}_3/\text{SBA-15}$  contained prominent peaks at  $1.1^\circ$  and other peaks at  $0.8^\circ$  and  $1.7^\circ$ . Those peaks were the typical characterization of the hexagonal three-dimensional form indicated iron oxide doping completely within mesoporous channels of SBA-15 after impregnation treatment, ultrasonic and microwave. The ordered structure of the parent SBA-15 silica was changed after modification process. However, the diffraction peak intensity of the mesoporous silica SBA-15 decreased after iron added due to the iron act as strong X-ray absorber<sup>22</sup>. The typical peak of iron on XRD indicate that the presence of Hematite ( $\text{Fe}_2\text{O}_3$ ) reinforced with spread elements of EDX data (Fig.5). However, the diffraction peak correlates to iron oxide which indicates not formed crystal phase of iron oxide with big enough size outside of the porous structure.

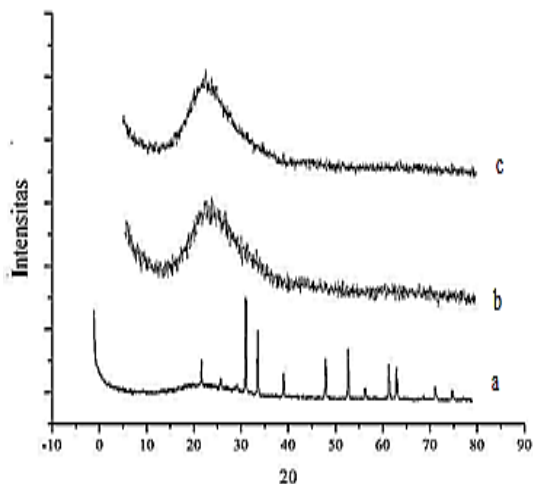


Fig. 2. The wide angle of XRD patterns of (a) Fe<sub>2</sub>O<sub>3</sub>, (b) SBA-15, and (c) Fe<sub>2</sub>O<sub>3</sub>/SBA-15

The curve of adsorption-desorption isotherm of mesoporous silica SBA-15 and iron modified on mesoporous silica SBA-15 showed by Fig.3. This isotherm generated by pore type of mesoporous silica SBA-15 as same well as IUPAC definition of type IV with H1 as hysteresis loop. The sharp inflection was shifted from P/Po 0.60 to 0.80 indicated the mesopore character range. Pore parameters for SBA-15 dan Fe<sub>2</sub>O<sub>3</sub>/SBA-15 are shown in Table. 1.

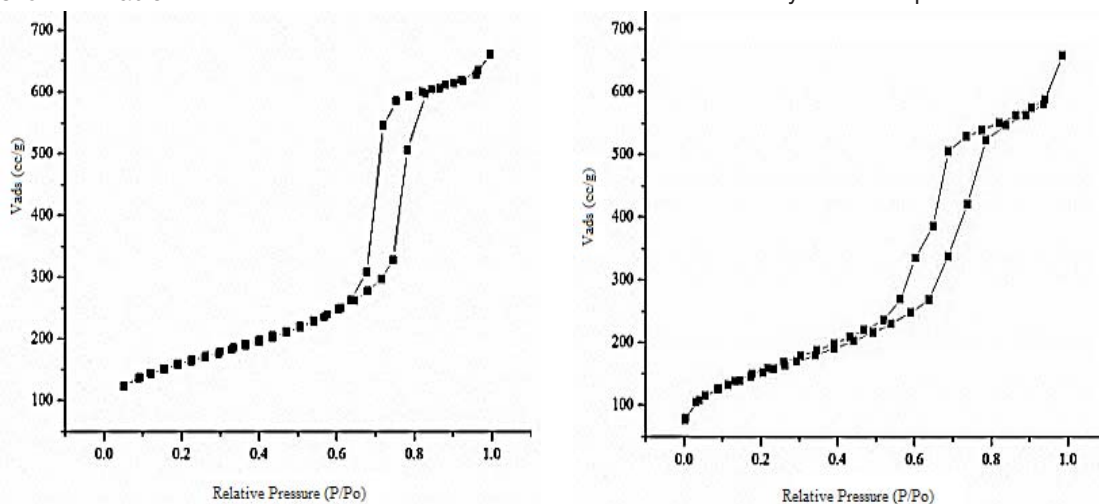


Fig. 3. Adsorption-desorption isotherm curve for (a) SBA-15, and (b) Fe<sub>2</sub>O<sub>3</sub>/SBA-15

Tabel. 1: Pore parameters for SBA-15 dan Fe<sub>2</sub>O<sub>3</sub>/SBA-15

Sample	S <sub>BET</sub> (m <sup>2</sup> g <sup>-1</sup> )	S <sub>BJH</sub> (m <sup>2</sup> g <sup>-1</sup> )	V <sub>BJH</sub> (cc g <sup>-1</sup> )	D <sub>BJH</sub> (nm)
SBA-15	556	515	1.02	8.68
Fe <sub>2</sub> O <sub>3</sub> /SBA-15	470	401	0.87	6.50

The BET surface area of SBA-15 and Fe<sub>2</sub>O<sub>3</sub>/SBA-15 decreased from 470 to 556 m<sup>2</sup>g<sup>-1</sup>. It also happens in the pore diameter and pore volume. Porosity parameter of asynthesized material such as specific surface area, pore size and volume was decrease due to the blocking pore of molecular sieve SBA-15 by Fe<sub>2</sub>O<sub>3</sub> particles during preparation process. The other reason came to the wet impregnation process that can be a stimulant for the blocking pore. These results indicate that the iron oxide was completely doping onto nanomaterial mesoporous silica SBA-15.

Figure. 4 show TEM image of Fe<sub>2</sub>O<sub>3</sub>/SBA-15 at different magnification. The general TEM image at perpendicular way describe the regular honeycomb framework as mesoporous silica structure. The iron particle which is labelled as black circle in TEM image (Fig. 4.a) show that iron has been successfully distributed on the surface of SBA-15. The other information from iron black circle section is the uniform size of disperse iron at range 0.5-1 nm without change the main structure of SBA-15. This result supported by FTIR, XRD, and BET. TEM and XRD data also show that the modification of SBA-15 with iron maintained the uniformity of molecular sieve mesoporous silica SBA-15 that described with the hexagonally structure of SBA-15 after all synthesis step.

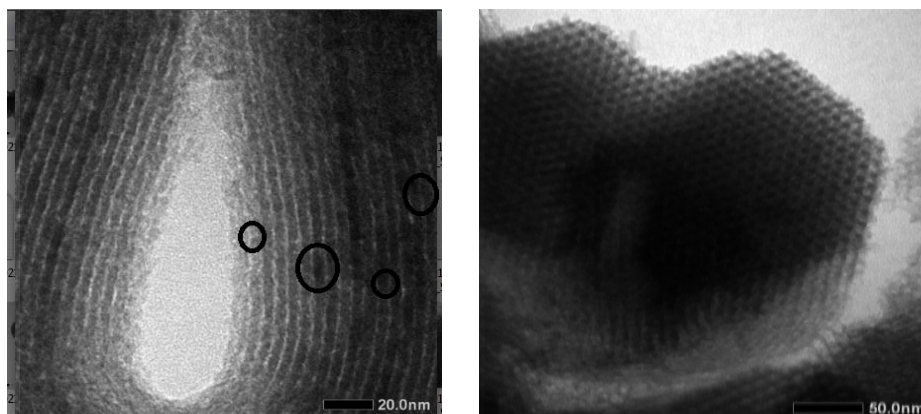


Fig. 4. TEM images of  $\text{Fe}_2\text{O}_3/\text{SBA-15}$  at (a) 20 nm and (b) 50 nm

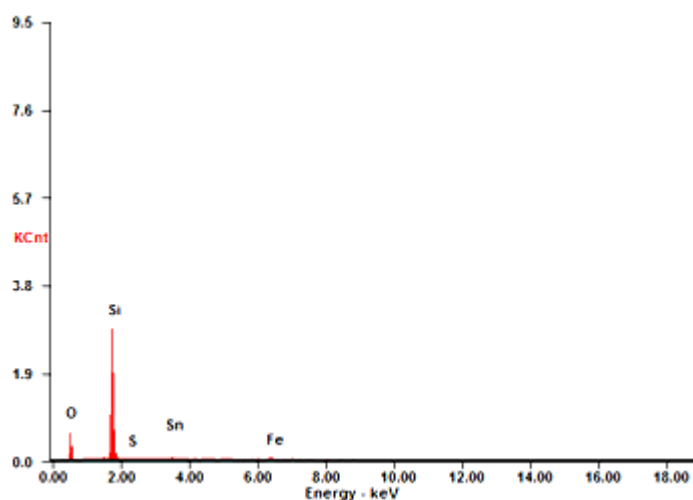


Fig. 5. EDX results for  $\text{Fe}_2\text{O}_3/\text{SBA-15}$

Figure. 5 show the result of elemental analysis of  $\text{Fe}_2\text{O}_3/\text{SBA-15}$  performed by EDX. The elemental identification by EDX explore that of SBA-15 mesoporous silica containing iron particle. Table 2 show that the iron content on  $\text{Fe}_2\text{O}_3/\text{SBA-15}$  adsorbent is 2.98%. The silica content record up to 50% which indicated that mesoporous silica SBA-15 act as good supporting material to produce  $\text{Fe}_2\text{O}_3/\text{SBA-15}$ . The other fact appear from the S and Sn element that predict as the impurity of precursor of iron. The iron doped within the mesoporous channels of SBA-15 indicates successful impregnation process according to the procedure. The results of EDX characterization is confirmed data from FTIR and X-Ray Diffraction (XRD).

**Table. 2: The element content of  $\text{Fe}_2\text{O}_3/\text{SBA-15}$  by Energy Dispersive X-Ray (EDX)**

Element	Weight (%)	Mass (%)
O	32.72	47.54
Si	60.72	50.26
S	00.49	00.35
Sn	03.10	00.61
Fe	02.98	01.24

Figure. 6 show the adsorption performance of  $\text{Fe}_2\text{O}_3/\text{SBA-15}$  when adsorbed nickel ion by conducted in isothermal condition at the room constant temperature. The time influence during nickel ion adsorption on  $\text{Fe}_2\text{O}_3/\text{SBA-15}$  to

adsorption capacity of sample are shown in Fig. 6. The adsorption of Ni (II) affected by the time contacts where the longer contact adsorbents will give the capacity of adsorption increases. The results indicate the optimum adsorption at the time of 240 min. contacting between Fe<sub>2</sub>O<sub>3</sub>/SBA-15 as

adsorbents and Ni (II) as adsorbate has reached equilibrium and evidenced by the adsorption capacity of samples tend to be constant after 240 minutes. This is due to the adsorption time of 240 min, Fe<sub>2</sub>O<sub>3</sub>/SBA-15 still active and not saturated yet by Ni (II) solutions.

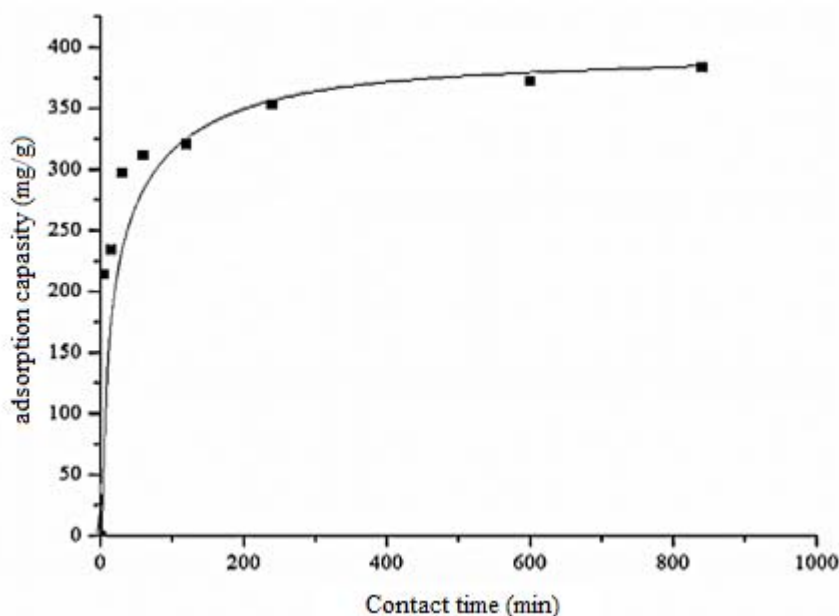


Fig. 6. Effect of time on adsorption capacity for Fe<sub>2</sub>O<sub>3</sub>/SBA-15

In this research, the equation of pseudo-first-order by Lagergren (2) and the pseudo-second-order by Ho and McKay (3) use as model of adsorption kinetic of the Fe<sub>2</sub>O<sub>3</sub>/SBA-15. The equation of both model described by follow section.

$$\ln\left(\frac{q_e}{q_e - q_t}\right) = Bt \quad (2)$$

$$\frac{t}{q_1} = \frac{1}{k_2 \cdot q_e^1} + \frac{1}{q_e} \cdot t \quad (3)$$

Where  $q_e$  (mg/g) is the amount of Ni (II) adsorbent upon reaching equilibrium,  $q_t$  (mg/g) is the amount of Ni (II) adsorbent at various times  $t$  (min.),  $(\text{min}^{-1})$  and  $k_2$  ( $\text{g}(\text{mg}/\text{min})^{-1}$ ) are the rate constants of the pseudo-first-order and the pseudo-second-order adsorption kinetic. In Table 3. It shows that the adsorption curve of Ni (II) on Fe<sub>2</sub>O<sub>3</sub>/SBA-15 suitable and follows the adsorption kinetics of the Lagergren Model because it has a higher linearity level than the Ho and McKay Models.

Table 3: Kinetics parameter for Ni (II) adsorption onto Fe<sub>2</sub>O<sub>3</sub>/SBA-15

Kinetic Models	Formula	Correlation coefficient (R <sup>2</sup> )	K
Lagergren	$\log(q_e - q_t) = \log q_e - kt$	0.948	0.0023
Ho and McKay	$2tkq_e^2 = \frac{q_e - q^1}{(q_e - qt)}$	0.142	0.0169

### CONCLUSION

The mesoporous silica of SBA-15 has been successfully modified with iron as an adsorbent for adsorption Ni (II) in wastewater. Mesoporous Fe<sub>2</sub>O<sub>3</sub>/SBA-15 has a regular amorphous structure obtained under test conditions with XRD instrument. Results show Fe<sub>2</sub>O<sub>3</sub>/SBA-15 keep the uniformity of hexagonal molecular sieve of SBA-15 structure after iron doping process. Decreasing pore surface area, pore diameter, and pore volume Fe<sub>2</sub>O<sub>3</sub>/SBA-15 compare with SBA-15 indicate that iron particles cover the the mesoporous channels of SBA-15. It also reinforced by EDX result that Fe content in Fe<sub>2</sub>O<sub>3</sub>/SBA-15 adsorbents is 2.98

wt%. The functional groups associated with the adsorbent show the Si-OH peak at the wavenumber, 1635.71 cm<sup>-1</sup> and the Si-O-Si group at the wavenumber, 1084.04 cm<sup>-1</sup>. The optimum capacity of Ni (II) adsorption reached 240 minutes at an initial Ni (II) concentration of 500 mg L<sup>-1</sup>. For suggestion, material mesoporous Fe<sub>2</sub>O<sub>3</sub>/SBA-15 could be develop as magnetic adsorbent for the future research.

### ACKNOWLEDGEMENT

Authors thanks the Sebelas Maret University for the funding support by Fundamental Research Grant PNPB Program 2018 (Contract Number 623/UN27.21/PP/2017)

### REFERENCES

- Dhokpande, S. R., Kaware, J. P., and Kulkarni, S. J. *International Journal of Science, Engineering and Technology Research.*, **2013**, 2,12, 2278–7798.
- Varma, S., Sarode, D., Wakale, S., Bhanvase, B. A, and Deosarkar, M. P. (2013). *International Journal of Chemical and Physical Science.s*, **2013**, 2, 132–139.
- Senthil Kumar, P., Ramakrishnan, K., and Gayathri, R. *Journal of Engineering Science and Technology.*, **2010**, 5(2), 234–245.
- Kundra R., Sachdeva R, A. S., and M., P., *J. Curr. Chem. Pharm. Sc*, **2012**, 2(1), 1–11.
- Turtureanu, A., Georgescu, C., and Oprean, L.. *Journal of Applied Sciences and Environmental Management.*, **2008**, 10(3), 159–162. <https://doi.org/10.4314/jasem.v10i3.17339>.
- Amuda, O., Amoo, I., Ipinmoroti, K., and Ajayi. *Journal of Applied Sciences and Environmental Managemen.t.*, **2006**, 10 (3), 159–162. <https://doi.org/10.4314/jasem.v10i3.17339>.
- Orbély, G. B., and Agy, E. N. *Journal of Applied Sciences and Environmental Management.*, **2008**, 10 (3), 159–162. <https://doi.org/10.4314/jasem.v10i3.17339>.
- Srivastava, N. K., and Majumder, C. B. (). *Journal of Hazardous Materials.*, **2008**, 151(1), 1–8. <https://doi.org/10.1016/j.jhazmat.2007.09.101>.
- Krishna, R. H., & Swamy, A., *Journal of Applied Sciences and Environmental Management.*, **2011**. 1-13.
- Varma, S., Sarode, D., Wakale, S., Bhanvase, B. and Deosarkar, M. P. *International Journal of Chemical and Physical Sciences*, 2( Special Issue)., **2013**, 132–139.
- Ulfa, M. Trisunaryanti, W. Falah, I. I. and Kartini, I. Indones. *J. Chem.*, 2016., 16(3) 239-242
- Ulfa, M, Setiawan, L. P. and Setyaningrum, A., *Orient. J. Chem.*, **2017**, 33(2) 829-834,.
- Taguchi, A. and Schuth F., *Microporous Mesoporous Mater.*, **2004**, 77, 1-45.
- Zhao, D., Wan, Y., dan Zhou, W., *Ordered Mesopororous Material*. Germany: Wiley. VchVerlag GmbH and Co. KgaA. **2013**.
- Zhao, J., Gao, F., Fu, W., Jin, W., Yang, P., and Zhao, D., *Chemical Communications.*, **2002**, 7, 752-753.
- Zhang, Y., Liu, R., Hu, Y., and Li, G. *Chemical Communications.*, **2009**. 81(3), 967–976. <https://doi.org/10.1021/ac8018262>.

17. Deng, Y., Yang, W., Wang, C., and Fu, S., *Advanced Materials.*, **2003**, 15(20), 1729–1732. <https://doi.org/10.1002/adma.200305459>.
18. Huang, H., Ji, Y., Qiao, Z., Zhao, C., He, J., and Zhang, H., *Journal of Automated Methods & Management in Chemistry.*, **2010**, 323-339. <https://doi.org/10.1155/2010/323509>
19. Vijayaraghavan, K., Jegan, J.R., and Velan, M., *Journal of Biotechnology.*, **2004**, 7(1), 61-71.
20. Viart, N., & Rehspringer, J.L. *Journal of Biotechnology.*, **2009**, 12(1), 1-11.
21. Amama, P.B., Lim, S., Ciuparu, D., Yang, Y., Pfefferle, L., and Haller, G.L., *Journal Physics Chemistry.*, **2005**, 109(7), 2645-2656.
22. Antonio, T.J.A., Jacome, C.M.A., Cerros, O.S.L., Palacios, M.E., Parra, S.R., Chavez, A.C., Navarete, J., & Salinas, L.E., *Applied Catalysis B: Environmental.*, **2010**, 100, 47-54.
23. Sing, K.S.W., Everett, D.H., Haul, R.A.W., . *Pure Applied Chemistry.*, **1985**, 57(4), 603-619.